Fluorescent sulphur and nitrogen containing porous polymers with tuneable donor-acceptor domains for light-driven hydrogen evolution

Dana Schwarz,[a,b] Amitava Acharja,[c] Arun Ichangi,[c] Pengbo Lyu,[d] Maksym V. Opanasenko,[d] Fabian R. Goßler,[b] Tobias A. F. König,[b] Jiří Čejka,[d] Petr Nachtigall,[d] Arne Thomas,[c] Michael J. Bojdys*[c,e]

Abstract: Light-driven water splitting is a potential source of abundant, clean energy, yet efficient charge-separation and size and position of the bandgap in heterogeneous photocatalysts are challenging to predict and design. Synthetic attempts to tune the bandgap of polymer photocatalysts classically rely on variations of the sizes of their π-conjugated domains. However, only donor-acceptor dyads hold the key to prevent undesired electron-hole recombination within the catalyst *via* efficient charge separation. Building on our previous success in incorporating electron-donating, sulphur-containing linkers and electron-withdrawing, triazine (C_3N_3) units into porous polymers, we report the synthesis of six visible-light active, triazine-based polymers with a high heteroatom-content of S and N that photocatalytically generate H_2 from water: up to 915 μmol h^{-1} g^{-1} with Pt co-catalyst, and – as one of the highest to-date reported values – 200 μmol h^{-1} g^{-1} without. The highly modular Sonogashira-Hagihara cross-coupling reaction we employ, enables a systematic study of mixed (S, N, C) and (N, C)-only polymer systems. Our results highlight that photocatalytic water-splitting does not only require an ideal optical bandgap of ~2.2 eV, but that the choice of donor-acceptor motifs profoundly impacts charge-transfer and catalytic activity.

Polymeric semiconductor photocatalysts for hydrogen evolution from water are an intriguing material class, since they can be produced from a continuous spectrum of variable monomers. This sets them apart from crystalline inorganic semiconductors that rely on very discrete compositions for bonding or catalytic activity to occur.[1] For example, conjugated microporous polymers (CMPs) can be prepared from statistical co-polymerisation of polycyclic, aromatic sub-units of varying sizes that enable pore-size tuning,[2] a continuous spectrum of bandgaps,[3] and as a result also varying degrees of photocatalytic activity.[4] The chemical make-up of the overwhelming majority of CMPs is carbon-only. As a consequence, charge-transfer is insufficient to prevent spontaneous recombination of photo-induced electron-hole pairs,[5] and efficient photocatalysis using CMPs strictly relies on electron migration to a noble-metal co-catalyst, usually platinum (Pt). In practice, nearly all photocatalytic water splitting studies explore one half-reaction – proton reduction – in a set-up that provides a sacrificial electron donor, such as triethanolamine (TEOA) and Pt as a co-catalyst. Cooper *et al.* pointed out that to make use of the full benefit of polymeric photocatalysts, the addition of Pt as a co-catalyst should not be essential.[4b] Conversely, polymeric carbon nitride has a very high stoichiometric ratio of carbon-to-nitrogen of 6-to-9. Although this polymer shows some, low activity in noble metal free photocatalysis, again only the addition of a Pt co-catalyst makes this process efficient.[6] Substantially higher hydrogen evolution rates are achieved predominantly *via* post-synthetic modifications of polymeric carbon nitrides by templating or by further heteroatom-doping.[7] In summary, it seems that introduction of distinct domains or point-defects increases the likelihood of electron-hole separation and thus of enhanced photocatalytic activity; a finding that was confirmed for azine covalent organic frameworks.[8] It is worth to note, that claims of no addition of a metal co-catalyst do not necessarily equate to a truly "metal-free" catalysis. Oftentimes, heavy metal ions and other elements (*e.g.* Pd, Cu, P) remain in the polymer matrix as residue from the linking reaction and have to be taken into account when comparing photocatalytic activity.[9]

There are ways of tuning surface polarity, pore structure, and catalytic properties of conjugate polymer frameworks for example by incorporation of the triazine (C_3N_3) group – an electron-withdrawing and spatially co-planar, C_3 symmetric building block.[10] We explored further modifications in a series of sulfur- and nitrogen-containing porous polymers (SNPs) that exploit donor-acceptor interactions for bandgap-tuning and charge separation for photocatalysis,[11] and one of these networks shows the highest reported hydrogen evolution rate under visible light irradiation for an as-received polymer photocatalyst to-date.[12] Inspired by the lead that incorporation of donor-acceptor domains holds the key to enhanced photocatalytic activity, here, we explore six covalent triazine-based porous polymer frameworks with subtle variation of their heteroatom content.

[a] Dr., D, Schwarz, A. Ichangi
Department of Organic Chemistry
Charles University
Hlavova 8, 128 43 Prague 2, Czech Republic
[b] Dr., D, Schwarz, F. R. Goßler, T. A. F. König
Leibniz-Institut fuer Polymerforschung Dresden e.V.,
Institute of Physical Chemistry and Polymer Physics,
Hohe Str. 6, 01069 Dresden, Germany
[c] A. Acharjya, Prof. Dr. Arne Thomas
Institute of Chemistry
Technische Universität Berlin
Hardenbergstraße 40, 10623 Berlin, Germany
[c] A. Ichangi, Dr. M. J. Bojdys
Institute of Organic Chemistry and Biochemistry of the CAS,
Flemingovo nám. 2, 166 10 Prague 6, Czech Republic
[d] Dr. M. V. Opanasenko, Prof. Dr. J. Čejka, P. Lyu, Prof. Dr. P. Nachtigall
Faculty of Science, Department of Physical and Macromolecular Chemistry
Charles University
Hlavova 8, 128 43 Prague 2, Czech Republic
[e] Dr. M. J. Bojdys
Humboldt-Universität zu Berlin
Department of Chemistry
Brook-Taylor-Str. 2, 12489 Berlin, Germany
E-mail: m.j.bojdys.02@cantab.net

Two principle groups of (S, N, C)- and (N, C)-containing porous polymers have been achieved referred to as SNPs and NPs, respectively. The network-forming reaction is the palladium-catalysed Sonogashira-Hagihara cross-coupling protocol.[13] Note, that the polymers contain a very low residual of Pd from the cross-coupling of 0.04 to 0.13 wt% (see below and in the Supporting Information). Hence, it is unlikely that the Pd contributes significantly to the observed hydrogen evolution rates in the presence of co-catalyst. After purification, the products NP-3 (based on anthracene linkers), NP-4, NP-5, NP-6 (based on asymmetric N-heterocycles), SNP-3, and SNP-4 (based on sulphur- and nitrogen-containing tectons) were obtained as yellow (NP-4, NP-5, and NP-6), orange (SNP-4) and brown (NP-3 and SNP-3) powders with yields above ~90% (see Scheme 1 and Figure S2). Experimental details are given in the supporting information.

The polymers were characterised by infrared (IR) spectroscopy, thermogravimetric analysis (TGA), ^{13}C cross-polarisation magnetic-angle spinning (CP/MAS) NMR spectroscopy, X-ray photoelectron spectroscopy (XPS), and combustion elemental analysis (EA) to confirm the structure and possible impurities from the synthesis (see Supporting Information). In ^{13}C CP/MAS NMR spectroscopy all materials show a peak at 172 ppm ascribed to the C_3N_3 ring (Figure 1). Peaks between 142 and 124 ppm are assigned to the sp^2 hybridised carbons (C–C and C–H) and carbons within the sulphur- and nitrogen-containing heterocycles. Quaternary carbons are visible around 124 ppm. Peaks at approx. 99 and 88 ppm are sp hybridised –C≡C– sites. All networks show two sp-hybridised –C≡C– environments due to asymmetric substitution across this bridge. IR spectra of all six polymers are shown in Figure S10 and reveal miniscule peaks at 3300 cm^{-1} that correspond to the unreacted –C≡C–H bond vibrations. The –C≡C– bond formed during the polymerisation shows as a peak at around 2200 cm^{-1}.[14] EA, EDX, and TGA confirm the yields of around 100% with almost no residual elements from the coupling reaction (*e.g.* residual Pd content varies between 0.04 to 0.13 wt%) (Table S4, S5, S6 and Figure S5). Similar Sonogashira and also Suzuki coupling reactions often lead to higher concentrations of residual catalyst.[13, 15]

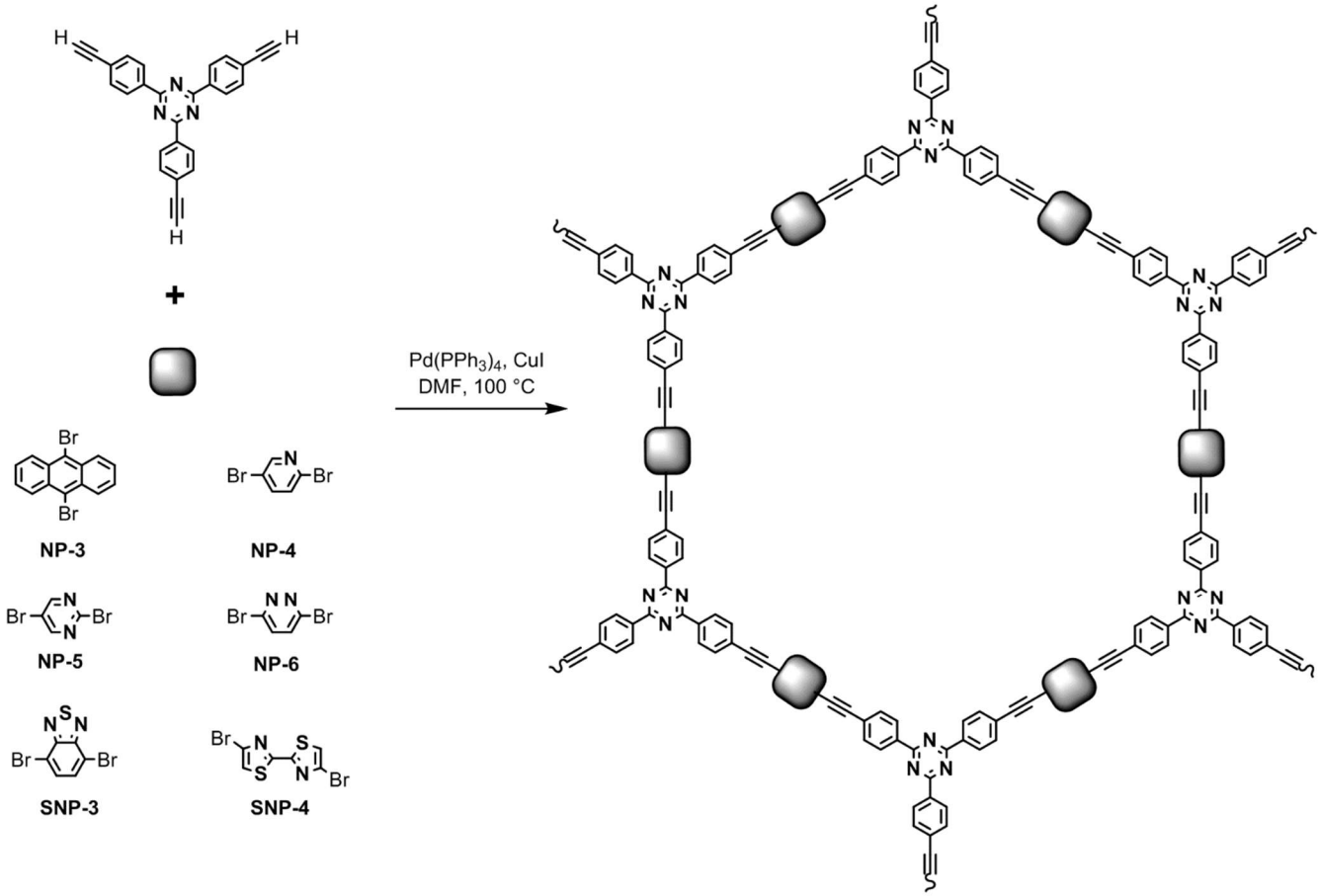

Scheme 1. Synthetic route to NPs and SNPs. C_3-symmetric 2,4,6-tris(4-ethynylphenyl)-1,3,5-triazine is coupled with a C_2-symmetric bridge such as: 9,10-dibromoanthracene to yield **NP-3**, 2,5-Dibromopyridine to yield **NP-4**, 2,5-dibromopyrimidine to yield **NP-5**, 3,6-dibromopyridazine to yield **NP-6**, 4,7-dibromobenzo-[c]-1,2,5thiadiazole to yield **SNP-3**, and 5,5'-dibromo-2,2'-bithiazole to yield **SNP-4**.

The pore systems of the polymers were investigated by nitrogen sorption measurements at 77 K (Figure 2a). All polymers feature micro- and mesopores with a visible hysteresis. The accessible surface areas calculated by Brunauer-Emmett-Teller (BET) equation are between 210 and 600 $m^2\ g^{-1}$ (Table 1) which is in the range of similar, carbon-only CMPs (*e.g.* CMP-3 with

522 m^2 g^{-1}).[13] In general, surface areas of previously reported S- and N-containing polymers are on average lower with values between 12 and 250 m^2 g^{-1}.[14-15, 16]

CO_2 uptake values are within the range of nitrogen-containing CMPs and show a dependence on overall nitrogen content and surface area.[2, 17] NP-5 and NP-6 have the highest amount of nitrogen and feature the highest CO_2 uptake with around 1.9 mmol g^{-1}. SNP-4 has the lowest CO_2 uptake with 1.30 mmol g^{-1} (similar to NP-3) due to the comparably low guest-accessible surface area. CO_2 sorption isotherms are shown in Figure 2b and show a linear uptake with no discernible hysteresis which is typical for microporous polymers.

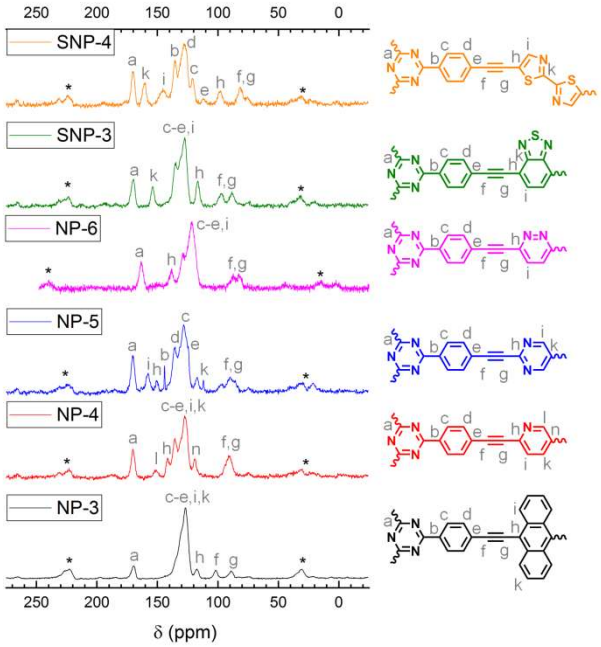

Figure 1. ^{13}C CP-MAS ssNMR spectra of NPs and SNPs from top to bottom **SNP-4** (in orange), **SNP-3** (in green), **NP-6** (in magenta), **NP-5** (in blue), **NP-4** (in red), and **NP-3** (in black). Spectra were recorded at a MAS rate of 12.0 kHz featuring triazine, phenyl and ethylene groups from left to right-hand-side, asterisks denote spinning sidebands.

Figure 3 shows scanning and transmission electron microscopy (SEM and TEM) images together with the corresponding selected area electron diffraction patterns (SAED). All networks have an intergrown, particle-like morphology. Remarkably, samples NP-3, NP5, NP-6 and SNP-4 feature pronounced Moiré fringes in their TEM images and/or electron diffraction spots indicative of some degree of internal order. Nonetheless, powder X-ray diffraction (PXRD) patterns reveal that the bulk of the samples is predominantly glassy and amorphous (Figure S6). Interlayer stacking peaks around 25° 2θ are observed and are comparable to other layered, aromatic systems such as CMPs and covalent organic frameworks (COFs).[18]

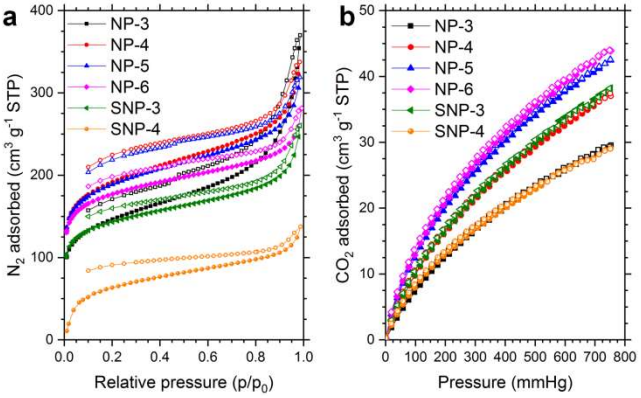

Figure 2. a) Nitrogen adsorption/desorption isotherms and b) CO_2 sorption isotherms measured at 273K for NP-3 (in black), NP-4 (in red), NP-5 (in blue), NP-6 (in magenta), SNP-3 (in green), SNP-4 (in orange). Data points in the adsorption and desorption branch of the isotherms are indicated by filled and empty circles, respectively

Table 1. Gas sorption data of all 6 polymers, including pore sizes and CO_2 uptake calculated from sorption isotherm.

Sample	S_{BET} (m^2 g^{-1})[a]	PV (cm^3 g^{-1})[b]	CO_2 uptake (mmol/g)
NP-3	468	0.643	1.32
NP-4	600	0.193	1.65
NP-5	590	0.223	1.89
NP-6	545	0.376	1.96
SNP-3	445	0.382	1.71
SNP-4	210	0.159	1.30

[a]Surface area calculated from N_2 adsorption isotherm using the BET equation. [b]Pore volume (PV) calculated from N_2 uptake for pore-sizes between 1.7 and 300 nm. Pore volume calculated *via* the Barrett-Joyner-Halenda (BJH) method.

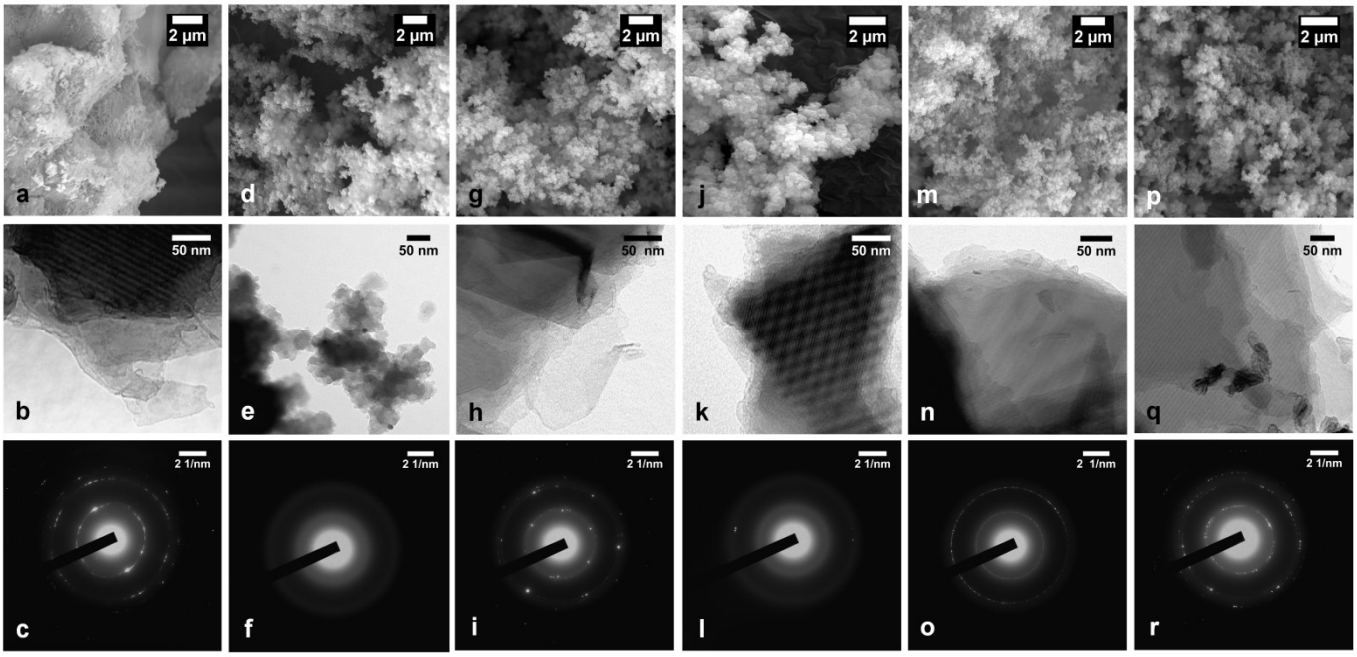

Figure 3. Electron microscopic investigation of SNPs. SEM (top), TEM (centre), and SAED (bottom) images for: a-c) NP-3, d-f) NP-4, g-i) NP-5, j-l) NP-6, m-o) SNP-3, and p-r) SNP-4. b, h and n) Networks NP-3, and NP-6 show Moiré fringes in TEM images indicative of overlapping, ordered layers. c, i, o and r) show concentric rings in the electron diffraction that are indicative of polycrystalline domains.

Solid-state UV/Vis spectra of the polymers were recorded at room temperature and are displayed in Figure S9. The direct band gaps were calculated using the Kubelka-Munk method (Figure S10) and vary between 1.9 and 2.52 eV and are in broad agreement with the calculated band structures (at PBE/DZP/GD2/5x5x16k-points level) of periodic, single layer structures of the corresponding materials (Figure S12). Photoluminescence emission (PLE) measurements show emission maxima in the range of 550 to 610 nm upon excitation at 405 nm (Figure 4b) as a result of the extended conjugation in the polymer network. Furthermore, the red shift implies the degree of near-perfect polymerisation which is in agreement with the low residual halogen content in the polymers (see ICP-analysis, SI).[19] NP-3 is the structure without heteroatoms except for the triazine bridge acceptor and features the highest red shift followed by SNP-3, SNP-4, and NP-6. Time-correlated fluorescence spectra were performed at 400 nm for NPs and SNPs in the solid state to investigate the dynamics of the excited-state (Figure 4c). The average fluorescence lifetimes are 1.49 (NP-3), 1.72 (NP-4), 1.69 (NP-5), 1.48 (NP-6), 1.29 (SNP-3), and 1.17 ns (SNP-4), and they were estimated by a double-exponential fitting. Excitons in NP-4 and NP-5 have the longest lifetime, and they are shortest in SNPs. Electron donation from sulphur heteroatoms may result in faster fluorescence quenching. An increase in N-content from pyridine- (NP-4) or pyrimidine-linkers (NP-5) leads to an increase in exciton lifetimes due to stronger C-H···N hydrogen bonds between adjacent layers. We have seen previously that it is not only the size of the π-conjugated organic tecton that determines the band gap of the resulting polymer but also the strength of donor-acceptor interactions within the network.[3, 20] In addition to charge-delocalisation between far-apart sulphur- and nitrogen-containing domains, the triazine-based ethynyl-phenyl linker features intrinsic donor-acceptor properties that can facilitate intramolecular charge transfer and, hence, exciton migration on a more local scale. As a result, all polymers with high nitrogen content (*i.e.* all NPs) can retain the excited state for a longer time. Indeed calculations suggest that the triazine ring has a larger hyperpolarisability and more electron-withdrawing character than the analogous carbon-only benzene core.[21]

All samples were investigated in photocatalytic hydrogen evolution from water using platinum (Pt) co-catalyst and triethanolamine (TEOA) as sacrificial agent under visible light (395 nm cut-off filter). Control reactions in the dark were performed prior to each test run to verify photocatalytic action. Figure 5 summarises the hydrogen evolution rates (HERs) for all samples with and without platinum as a co-catalyst in dependence of the calculated, direct optical band gap. NP-5 has the highest HER with Pt at 915±10 µmol h^{-1} g^{-1} (9.15±0.1 µmol h^{-1}) and 200±10 µmol h^{-1} g^{-1} (2.00±0.1 µmol h^{-1}) without additional co-catalyst; one of the highest HER values for a noble metal free photocatalyst to-date. Common benchmark polymeric photocatalysts based on organic nitrogen rich moieties are heptazine based polymers[22] such as pure g-CN [23], CNC_{30} (with cytosine) [23], B-modified g-CN [24], poly(triazine imide)[25] and azine-based COFs [26]. At first glance, we see a similar trend to previous publications that an ideal optical band gap for efficient photocatalysis is situated around 2.2 eV,[4b, 11] and that band gaps below 2.0 eV fail to catalyse the reaction presumably because they are too narrow to straddle the potential between proton reduction and oxidation of the sacrificial agent. However, we also observe a (weak) correlation of HER and guest-accessible surface area with more accessible pore structures achieving

higher efficiencies (Figure S28). The highest HER values with platinum as co-catalyst were obtained for pyridine (NP-4) and pyrimidine (NP-5) as a tecton. However, within the group of NPs

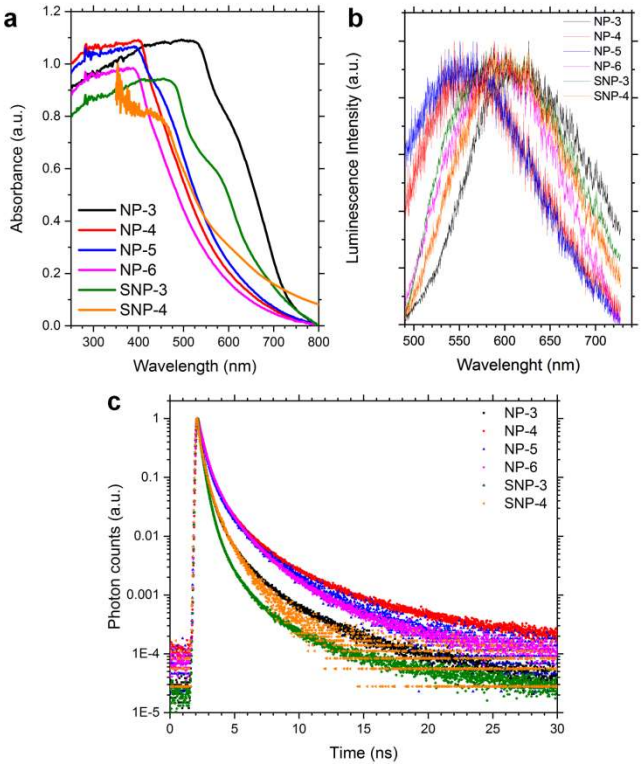

Figure 4. a) Absorbance, b) fluorescence spectra, and c) time-correlated fluorescence spectroscopy for SNPs and NPs with **SNP-4** (in orange), **SNP-3** (in green), **NP-6** (in magenta), **NP-5** (in blue), **NP-4** (in red), and **NP-3** (in black).

HER (Figure S29), and hence, we assume that it is the position of heteroatoms in the frameworks (rather than their sheer amount) that has the most impact on donor-acceptor interactions, charge-delocalisation and photocatalytic activity. In the light of the PLE study, we observe the trend that long exciton life-times in NPs are a good indicator for efficient photocatalysis, most likely, because photoexcited electrons and holes do not spontaneously recombine so readily in these materials.

In conclusion, we have expanded the family of sulphur- and nitrogen-containing porous polymers – a class of photoactive, heterogeneous catalysts – by six further members with mixed (S, N, C) and (N, C)-only heteroatoms in their backbones. Intrinsic donor-acceptor interactions within these networks allow fine-tuning of the optical bandgap between 1.90 and 2.57 eV. Surprisingly, we find that efficient photocatalytic hydrogen evolution from water does not only depend on the optimal size of the bandgap (~ 2.2 eV) – as suggested in previous reports. We find that materials that effectively extend the life-time of the photoexcited electron-hole pair – for example *via* effective charge separation – can achieve high hydrogen evolution rates irrespective at sub-optimal bandgap values. In conventional systems that do not feature intrinsic donor-acceptor dyads, this the pyridazine tecton (NP-6) has a low HER. Overall, the absolute heteroatom content did not show any correlation with

electron-hole separation needs to be promoted by the addition of Pt or Pd co-catalysts (Figure S30). Thus, we achieve hydrogen evolution rates of up to 200±10 μmol h^{-1} g^{-1} without co-catalyst which is one of the highest values reported to date. This is a significant finding and we believe that it highlights the importance of tuneable donor-acceptor domains in the development of a truly noble metal free photocatalyst in the future.

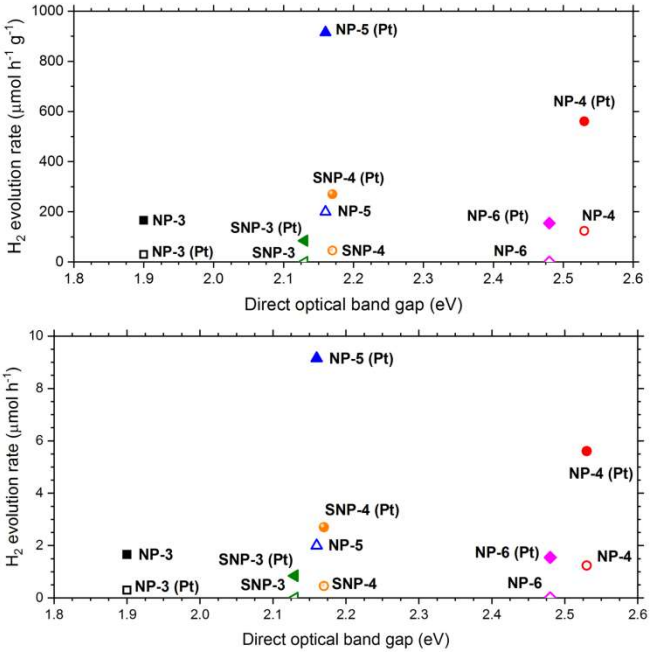

Figure 5. Hydrogen evolution rates of NP-3, NNPs, and SNPs (10 mg) under visible light (395 nm cut-off filter) correlated with the direct optical band gap in μmol h^{-1} g^{-1} (above) and μmol h^{-1} (below). Each measurement was performed in a water:acetonitrile (1:1) mixture using triethanolamine (TEOA) as sacrificial agent with 3 wt% platinum (Pt) (filled symbols) and without Pt co-catalyst (empty symbols). Corresponding solid-state UV/Vis diffuse-reflectance spectra are shown in Figure S9.

Acknowledgements

We thank Dr. Nikolai Makukhin for discussions, Šárka Pšondrová is acknowledged for IR, Dr. Simona Hybelbauerova and Martin Dracinsky for their support and access in solid-state NMR, Dr. Jiri Rybacek and Dr. Martin Racek for their support in SEM and EDX, Stanislava Matejkova.is acknowledged for ICP-OES, Jaroslava Hnilickova is acknowledged for EA and Christina Eichenauer is acknowledged for BET. M.J.B. thanks the European Research Council (ERC) for funding under the Starting Grant scheme (BEGMAT – 678462). M.J.B., J.C. and P.N. further acknowledge the Charles University Centre of Advanced Materials (CUCAM) (OP VVV Excellent Research Teams, project number CZ.02.1.01/0.0/0.0/15_003/0000417).

Keywords: conjugated microporous polymers • donor-acceptor dyads • triazine • photocatalysis

References

[1] aL. Yang, H. Zhou, T. Fan, D. Zhang, *Physical Chemistry Chemical Physics* **2014**, *16*, 6810-6826; bX. Chen, S. Shen, L. Guo, S. S. Mao, *Chemical Reviews* **2010**, *110*, 6503-6570.

[2] J.-X. Jiang, F. Su, A. Trewin, C. D. Wood, H. Niu, J. T. A. Jones, Y. Z. Khimyak, A. I. Cooper, *Journal of the American Chemical Society* **2008**, *130*, 7710-7720.

[3] J.-X. Jiang, A. Trewin, D. J. Adams, A. I. Cooper, *Chemical Science* **2011**, *2*, 1777-1781.

[4] aR. S. Sprick, B. Bonillo, R. Clowes, P. Guiglion, N. J. Brownbill, B. J. Slater, F. Blanc, M. A. Zwijnenburg, D. J. Adams, A. I. Cooper, *Angewandte Chemie* **2016**, *128*, 1824-1828; bR. S. Sprick, J.-X. Jiang, B. Bonillo, S. Ren, T. Ratvijitvech, P. Guiglion, M. A. Zwijnenburg, D. J. Adams, A. I. Cooper, *Journal of the American Chemical Society* **2015**, *137*, 3265-3270.

[5] G. Pierre, B. Cristina, Z. M. A., *Macromolecular Chemistry and Physics* **2016**, *217*, 344-353.

[6] X. Wang, K. Maeda, A. Thomas, K. Takanabe, G. Xin, J. M. Carlsson, K. Domen, M. Antonietti, *Nat Mater* **2009**, *8*, 76-80.

[7] F. K. Kessler, Y. Zheng, D. Schwarz, C. Merschjann, W. Schnick, X. Wang, M. J. Bojdys, **2017**, *2*, 17030.

[8] V. S. Vyas, F. Haase, L. Stegbauer, G. Savasci, F. Podjaski, C. Ochsenfeld, B. V. Lotsch, *Nature Communications* **2015**, *6*, 8508.

[9] aY. Wang, X. Wang, M. Antonietti, *Angewandte Chemie International Edition* **2012**, *51*, 68-89; bL. Li, W.-y. Lo, Z. Cai, N. Zhang, L. Yu, *Macromolecules* **2016**, *49*, 6903-6909.

[10] aR. Fink, C. Frenz, M. Thelakkat, H.-W. Schmidt, *Macromolecules* **1997**, *30*, 8177-8181; bH. Meier, E. Karpuk, H. Christof Holst, *European Journal of Organic Chemistry* **2006**, *2006*, 2609-2617; cI. Nenner, G. J. Schulz, *The Journal of Chemical Physics* **1975**, *62*, 1747-1758; dK. M. Omer, S.-Y. Ku, Y.-C. Chen, K.-T. Wong, A. J. Bard, *Journal of the American Chemical Society* **2010**, *132*, 10944-10952; eY. Oumi, Y. Kakinaga, T. Kodaira, T. Teranishi, T. Sano, *Journal of Materials Chemistry* **2003**, *13*, 181-185; fS. Ren, Q. Fang, F. Yu, D. Bu, *Journal of Polymer Science Part A: Polymer Chemistry* **2005**, *43*, 6554-6561; gS. Ren, D. Zeng, H. Zhong, Y. Wang, S. Qian, Q. Fang, *The Journal of Physical Chemistry B* **2010**, *114*, 10374-10383; hT. Yamamoto, S. Watanabe, H. Fukumoto, M. Sato, T. Tanaka, *Macromolecular Rapid Communications* **2006**, *27*, 317-321; iL. Zou, Y. Fu, X. Yan, X. Chen, J. Qin, *Journal of Polymer Science Part A: Polymer Chemistry* **2008**, *46*, 702-712; jL. Zou, Y. Liu, N. Ma, E. Macoas, J. M. G. Martinho, M. Pettersson, X. Chen, J. Qin, *Physical Chemistry Chemical Physics* **2011**, *13*, 8838-8846; kL. Zou, Z. Liu, X. Yan, Y. Liu, Y. Fu, J. Liu, Z. Huang, X. Chen, J. Qin, *European Journal of Organic Chemistry* **2009**, *2009*, 5587-5593.

[11] D. Schwarz, Y. S. Kochergin, A. Acharjya, A. Ichangi, M. V. Opanasenko, J. Čejka, U. Lappan, P. Arki, J. He, J. Schmidt, P. Nachtigall, A. Thomas, J. Tarábek, M. J. Bojdys, *Chemistry – A European Journal* **2017**, *23*, 13023-13027.

[12] K. Yaroslav S., S. Dana, A. Amitava, I. Arun, K. Ranjit, E. Pavla, V. Jaroslav, S. Johannes, T. Arne, B. Michael J., *Exploring the "Goldilocks Zone" of Semiconducting Polymer Photocatalysts via Donor-Acceptor Interactions*, **2018**.

[13] J.-X. Jiang, F. Su, A. Trewin, C. D. Wood, N. L. Campbell, H. Niu, C. Dickinson, A. Y. Ganin, M. J. Rosseinsky, Y. Z. Khimyak, A. I. Cooper, *Angewandte Chemie International Edition* **2007**, *46*, 8574-8578.

[14] S. Ren, R. Dawson, D. J. Adams, A. I. Cooper, *Polymer Chemistry* **2013**, *4*, 5585-5590.

[15] aP. Guiglion, C. Butchosa, M. A. Zwijnenburg, *Macromol. Chem. Phys.* **2016**, *217*, 344-353; bH. Bildirir, J. P. Paraknowitsch, A. Thomas, *Chemistry – A European Journal* **2014**, *20*, 9543-9548.

[16] aK. Kailasam, M. B. Mesch, L. Möhlmann, M. Baar, S. Blechert, M. Schwarze, M. Schröder, R. Schomäcker, J. Senker, A. Thomas, *Energy Technology* **2016**, *4*, 744-750; bK. Zhang, D. Kopetzki, P. H. Seeberger, M. Antonietti, F. Vilela, *Angewandte Chemie International Edition* **2013**, *52*, 1432-1436; cH. Bohra, S. Y. Tan, J. Shao, C. Yang, A. Efrem, Y. Zhao, M. Wang, *Polymer Chemistry* **2016**, *7*, 6413-6421; dA. Efrem, K. Wang, P. N. Amaniampong, C. Yang, S. Gupta, H. Bohra, S. H. Mushrif, M. Wang, *Polymer Chemistry* **2016**, *7*, 4862-4866.

[17] R. S. Sprick, B. Bonillo, M. Sachs, R. Clowes, J. R. Durrant, D. J. Adams, A. I. Cooper, *Chemical Communications* **2016**, *52*, 10008-10011.

[18] P. Kuhn, M. Antonietti, A. Thomas, *Angewandte Chemie International Edition* **2008**, *47*, 3450-3453.

[19] F. D. T. M., S. S. C., W. Manfred, D. S. I., Z. K. A., M. Klaus, *Angewandte Chemie International Edition* **2008**, *47*, 10175-10178.

[20] aY. Xu, A. Nagai, D. Jiang, *Chemical Communications* **2013**, *49*, 1591-1593; bP. Dai, L. Yang, M. Liang, H. Dong, P. Wang, C. Zhang, Z. Sun, S. Xue, *ACS Applied Materials & Interfaces* **2015**, *7*, 22436-22447.

[21] V. R. Thalladi, S. Brasselet, H.-C. Weiss, D. Bläser, A. K. Katz, H. L. Carrell, R. Boese, J. Zyss, A. Nangia, G. R. Desiraju, *Journal of the American Chemical Society* **1998**, *120*, 2563-2577.

[22] W. Yong, W. Xinchen, A. Markus, *Angewandte Chemie International Edition* **2012**, *51*, 68-89.

[23] Y. Can, W. Bo, Z. Linzhu, Y. Ling, W. Xinchen, *Angewandte Chemie International Edition* **2017**, *56*, 6627-6631.

[24] L. Zhenzhen, W. Xinchen, *Angewandte Chemie International Edition* **2013**, *52*, 1735-1738.

[25] L. Lin, C. Wang, W. Ren, H. Ou, Y. Zhang, X. Wang, *Chemical Science* **2017**, *8*, 5506-5511.

[26] S. Katharina, T. Brian, M. M. B., W. Eva, M. Charlotte, T. Francis, S. Wolfgang, S. Jürgen, L. B. V., *Angewandte Chemie International Edition* **2013**, *52*, 2435-2439.